

Dynamics of optical gain in $\text{In}_x\text{Ga}_{1-x}\text{N}$ multi-quantum-well-based laser diodes

Yoichi Kawakami,^{a)} Yukio Narukawa, Kunimichi Omae, and Shigeo Fujita

Department of Electronic Science and Engineering, Kyoto University, Kyoto 606-8501, Japan

Shuji Nakamura^{b)}

Department of Research and Development, Nichia Chemical Industries Ltd., 491 Oka, Kaminaka, Anan, Tokushima 774-8601, Japan

(Received 30 May 2000; accepted for publication 8 August 2000)

Dynamical behavior of optical gain formation has been assessed at room temperature in the $\text{In}_x\text{Ga}_{1-x}\text{N}$ multi-quantum-well (MQW) based laser diodes (LDs) by employing pump and probe spectroscopy with a pulse width of 150 fs. The LDs are composed of (a) $\text{In}_{0.1}\text{Ga}_{0.9}\text{N}$ – $\text{In}_{0.02}\text{Ga}_{0.98}\text{N}$ MQW and (b) $\text{In}_{0.3}\text{Ga}_{0.7}\text{N}$ – $\text{In}_{0.05}\text{Ga}_{0.95}\text{N}$ MQW, whose stimulated emissions correspond to near ultraviolet (390 nm) and blue (440 nm), respectively. The optical gain was contributed from the nearly delocalized states [the lowest-quantized MQW levels (LQL)] in the sample (a), while it was from highly localized levels with respect to the LQL by 500 meV for the sample (b). It was found that the photogenerated carriers rapidly (less than 1 ps) transferred to the LQL, and then relaxed to the localized tail within the time scale of about 5 ps, giving rise to the optical gain. Such gain spectra were saturated and other bands appeared in the vicinity of the LQL under higher photoexcitation.

© 2000 American Institute of Physics. [S0003-6951(00)03240-X]

Recent development of the fabrication technology has opened the way to the commercialization of violet laser diodes (LDs),^{1,2} which are composed of InGaN/GaN/AlGaIn-based heterostructures. The tuning wavelength for the stable continuous-wave (cw) operation of LDs is currently in the range between 376 nm (Ref. 3) and 450 nm,⁴ which is much narrower than that of light-emitting diodes due to dramatic increase of I_{th} with increasing emission wavelength from 420 to 450 nm. This may be because the internal electric field is so large in In-rich active layers that oscillator strength between electron and hole is suppressed, and/or because the optical gain cannot be generated sufficiently due to the inhomogeneous broadening effect resulting in the limited number of density of states. Further breakthrough is, therefore, required to realize pure blue and green LDs using InGaIn-based semiconductors. Such targets can be facilitated by the well understanding of the emission mechanism, as well as by the well designing of LD structures.

So far, the assessment of stimulated emission has been reported in InGaIn multi-quantum-well (MQW) structures.^{5–10} However, the mechanism is still controversial, where some groups claim that carrier localization plays a key role in both spontaneous and stimulated emissions,^{5–7} while another one reports that localized states are saturated and delocalized states of electron–hole pairs contribute to the optical gain.⁸ Such discrepancy is probably because the degree of localization in InGaIn active layers differs according to both the mean In-mole fraction and growth conditions, resulting in the difficulty in the general discussion on optical properties.

In this letter, the dynamics of gain formation is studied

in a series of InGaIn MQW LDs whose wavelength of stimulated emissions corresponds to near ultraviolet (390 nm) and blue (440 nm) by employing pump and probe spectroscopy.

Two types of LD structures, whose In content in the active layers are roughly (a) 10% and (b) 30% are assessed in this study.^{4,6,11–13} Whole samples¹⁴ consist of a separate confinement heterostructure where (a) a Si-doped $\text{In}_{0.1}\text{Ga}_{0.9}\text{N}$ (3 nm)/ $\text{In}_{0.02}\text{Ga}_{0.98}\text{N}$ (6 nm) MQW with three periods and (b) an undoped $\text{In}_{0.3}\text{Ga}_{0.7}\text{N}$ (3 nm)/ $\text{In}_{0.05}\text{Ga}_{0.95}\text{N}$ (10 nm) MQW with six periods are sandwiched between GaN waveguide layers (0.1 μm in each) and $\text{Al}_{0.15}\text{Ga}_{0.85}\text{N}$ cladding layers (0.4 μm in each). The top of the $\text{Al}_x\text{Ga}_{1-x}\text{N}$ clad and the GaN waveguide are Mg-doped p -type layers, while the bottom of the clad and the waveguide are Si-doped n -type layers. The LD operation at room temperature (RT) was performed at 390 nm under cw mode for sample (a) (near-UV LD) and at 440 nm under pulsed mode for sample (b) (blue LD).

The pump and probe spectroscopy depicted was performed for the measurement of temporal behavior of differential absorption using a dual photodiode array in conjunction with a 25 cm monochromator.¹⁵ The white light used for the probe beam was generated by focusing part of the output beam from the regenerative amplifier on a D_2O cell. The pulse width of both the pump and probe beam was 150 fs. Delay time of the probe beam with respect to the pump beam was tuned by changing the position of the retroreflector which could be controlled by the pulse stage. In order to detect the probe beam with spatially uniform carrier distribution in the sample, the focus size of the pump beam (600 μm in diameter) was set so as to be much larger than that of the probe beam (200 μm in diameter). Furthermore, the probe beam was perpendicularly polarized with respect to the pump beam, and the transmitted probe beam polarized in this direction was detected to avoid the scattered component

^{a)}Electronic mail: kawakami@kuee.kyoto-u.ac.jp

^{b)}Present address: Materials Department, University of California, Santa Barbara, CA 93106.

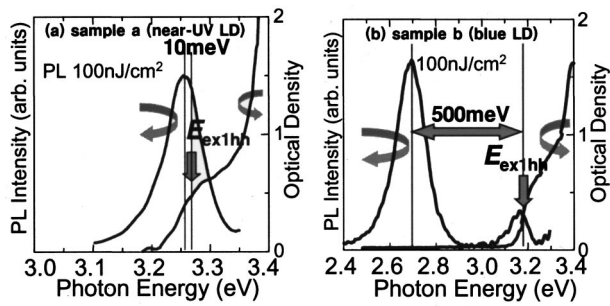


FIG. 1. Time-integrated PL under $I_{\text{ex}} = 100 \text{ nJ/cm}^2$ and optical density spectra under low photoexcitation energy density taken at (a) sample (a) ($\text{In}_{0.1}\text{Ga}_{0.9}\text{N}/\text{In}_{0.02}\text{Ga}_{0.98}\text{N}$ -MQW near-UV LD) and (b) sample (b) ($\text{In}_{0.3}\text{Ga}_{0.7}\text{N}/\text{In}_{0.05}\text{Ga}_{0.95}\text{N}$ -MQW blue LD).

of the pump beam. The whole measurements have been done at RT.

In the pump and probe spectroscopy, the transmission spectrum of the probe beam detected in the presence of the pump beam ($T + \Delta T$) is compared to the spectrum without the pump beam (T), giving the frequency (ω)-dependent $\Delta T(\omega, I_{\text{ex}}, t_d)$ of the sample for different intensities of the pump (I_{ex}), and for different time delays after the pulsed pumping (t_d). The photoinduced change of optical density [$\Delta \text{OD}(\omega, I_{\text{ex}}, t_d)$],

$$\Delta \text{OD} = \log\left(\frac{T}{T + \Delta T}\right) = \Delta \alpha d \times 0.434, \quad (1)$$

where $\Delta \alpha(\omega, I_{\text{ex}}, t_d)$ is the photoinduced change of absorption coefficient and d is the thickness of absorbing layer.

Figure 1 shows time-integrated photoluminescence (TI-PL) spectra under photoexcitation energy density (I_{ex}) of 100 nJ/cm^2 taken at two types of LDs. Absorption spectra under low photoexcitation (Xe lamp) corresponding to the density of states are also depicted in Fig. 1. The lowest quantized energy levels within the wells (designated as E_{ex1hh}) were estimated by electroreflectance spectroscopy. In contrast to sample (a), the PL of sample (b) is composed of two emission bands, and the main bands are located on the low-energy side with respect to E_{ex1hh} by 500 meV . Blueshift of

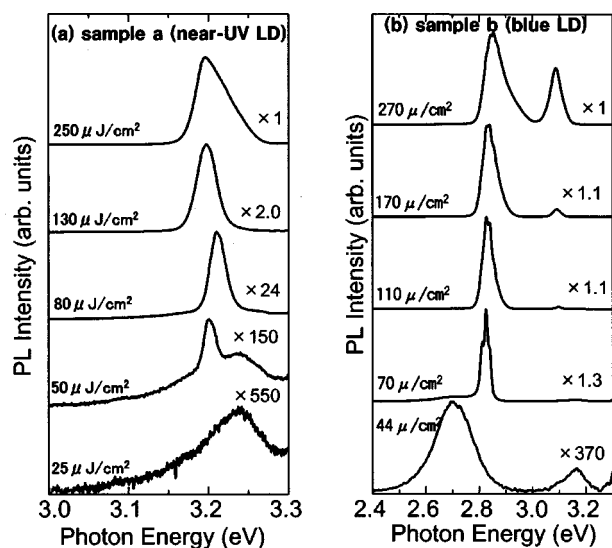


FIG. 2. Time-integrated PL from the resonator as a function of excitation energy density taken at (a) sample (a) and (b) sample (b).

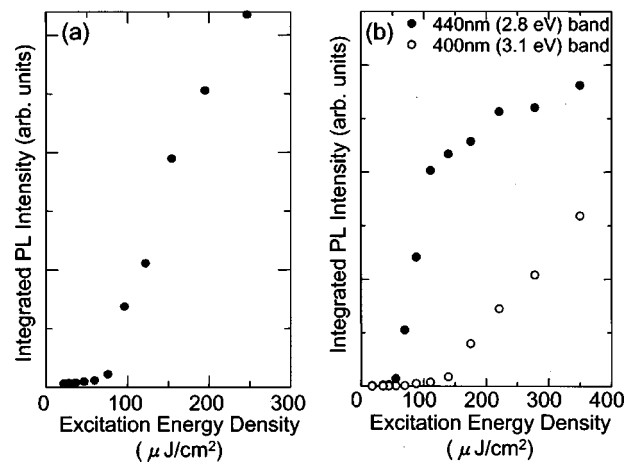


FIG. 3. Integrated PL intensity for the emission bands as a function of excitation energy density taken at (a) sample (a) and (b) sample (b).

these bands under increased I_{ex} conditions (from 10 nJ/cm^2 to $20 \mu\text{J/cm}^2$) is about a few tens meV, which is substantially smaller than the energy difference. These phenomena were attributed to the localization of excitons whose origin is probably due to In-rich quantum dot (QD) like centers. This model is supported by the energy-dispersive x-ray microanalysis using scanning transmission electron microscopy.⁵ Moreover, the zero-dimensional feature of excitons is revealed especially in blue-emitting quantum wells (QWs) where almost no temperature dependence of the radiative lifetime was observed from cryogenic temperature to RT.¹³

The TI-PL spectra were detected with the edge geometry from the resonator cavity—the length of which was about 1 mm . As shown in Figs. 2 and 3, stimulated emission (SE) was observed from every sample if I_{ex} is more than about $50 \mu\text{J/cm}^2$. SE appears on the low-energy side of the spontaneous emission (SPE) by 32 meV for sample (a), while from the high-energy side of the main SPE band by 130 meV for sample (b). The Large blueshift in sample (b) may be due to the band-filling effects within localized states, and/or due to the screening effect of the internal electric field. Nevertheless, this energy is still substantially smaller than the localization energy (500 meV) observed in the SPE. Therefore, it is probable that the optical gain was contributed from the localized centers for the blue LD mean-In composition of which in the wells is about 30%. However, as shown in Fig. 3(b), these SE bands are saturated if I_{ex} is more than about $100 \mu\text{J/cm}^2$, then new SE bands grow on the low-energy side of the SPE bands originating from the E_{ex1hh} transition.

The dynamical behavior of dense carriers was characterized by measurement of the differential absorption coefficient by employing pump and probe spectroscopy. Figure 4(a) shows the variation of differential optical density spectra as a function of time after pumping at 370 nm under $I_{\text{ex}} = 200 \mu\text{J/cm}^2$ in sample (a) ($\text{In}_{0.1}\text{Ga}_{0.9}\text{N}$ QW, near-UV LD). The optical density spectrum taken under the low I_{ex} condition is depicted as a reference. PL spectra of both SE ($I_{\text{ex}} = 200 \mu\text{J/cm}^2$) and SPE ($I_{\text{ex}} = 100 \text{ nJ/cm}^2$) taken from the surface are also shown in Fig. 4(a). The sheet carrier density is roughly estimated to be $1.9 \times 10^{13} \text{ cm}^{-2}$ under $I_{\text{ex}} = 200 \mu\text{J/cm}^2$. At the initial stage of excitation ($t =$

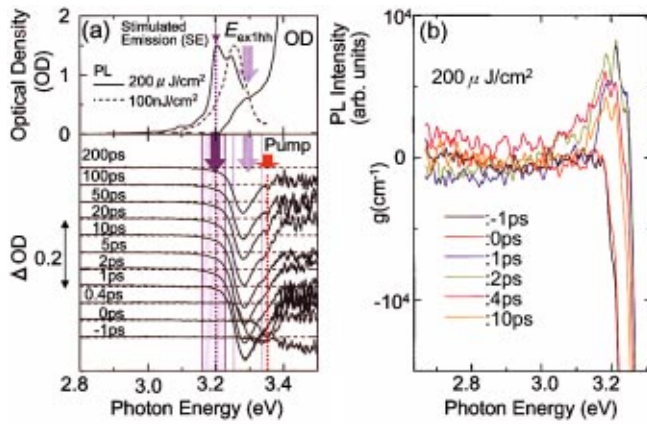


FIG. 4. (Color) (a) Differential optical density spectra as a function of time delay under $I_{ex}=200 \mu\text{J}/\text{cm}^2$ taken at sample (a) (near-UV LD). Optical density (OD) spectrum taken under low photoexcitation energy density, as well as PL spectra taken from the surface under $I_{ex}=100 \text{ nJ}/\text{cm}^2$ [spontaneous emission (SPE)] and 200 under $I_{ex}=200 \mu\text{J}/\text{cm}^2$ [stimulated emission (SE)] are depicted in the figure. (b) Dynamics of optical gain evaluated by the data in (a).

–0.5–0 ps), bleaching of the photoabsorption was observed in the vicinity of the pumping energy. However, the negative peak of ΔOD rapidly reached the level of E_{ex1hh} at a time scale of less than 1 ps. The red shift of E_{ex1hh} was observed with increasing time (13 meV at $t=200$ ps), probably because screening of the piezoelectric field is reduced with decreasing carrier density.¹⁶ Optical gain was generated on the low-energy side of the negative peak due to the effect of band-gap renormalization. As shown in Fig. 4(b), maximum optical gain as large as about 8000 cm^{-1} was reached at $t=2$ ps.

The dynamics of dense carriers was also assessed for sample (b) (blue LD), as shown in Fig. 5(a). The tail of differential absorption began to grow toward the bottom of the localized levels just after the bleaching at E_{ex1hh} is completed. The time scale for reaching to the bottom was about 5 ps. Therefore, it was found that photogenerated carriers and/or excitons efficiently transfer to deeply localized levels without the effect of a phonon bottleneck observed in other QD systems. As described before, stimulated emission originating from localized centers [designated as SE_1 in Fig. 5(a)] saturates under higher photoexcitation, and a new SE from E_{ex1hh} (SE_2) appears in these samples. Figure 5(b) shows the dynamics of optical gain spectra under $I_{ex}=200 \mu\text{J}/\text{cm}^2$ taken at sample (b) (blue LD). SE_2 began to grow at $t=1$ –2 ps and reached the maximum ($g=3000 \text{ cm}^{-1}$) at $t=4$ ps, while the temporal behavior of SE_1 is delayed by about 2 ps with respect to that of SE_2 .

In conclusion, the dynamics of dense carriers has been studied at RT in (a) $\text{In}_{0.1}\text{Ga}_{0.9}\text{N}/\text{In}_{0.02}\text{Ga}_{0.98}\text{N}$ and (b) $\text{In}_{0.3}\text{Ga}_{0.7}\text{N}/\text{In}_{0.05}\text{Ga}_{0.95}\text{N}$ MQW LD structures by means of pump and probe spectroscopy. The optical gain was contributed from the nearly delocalized state of the QW (E_{ex1hh}) in sample (a). However, it was generated from both QD-like localized centers and the QW under moderately high photoexcitation in sample (b). It was found that the photogener-

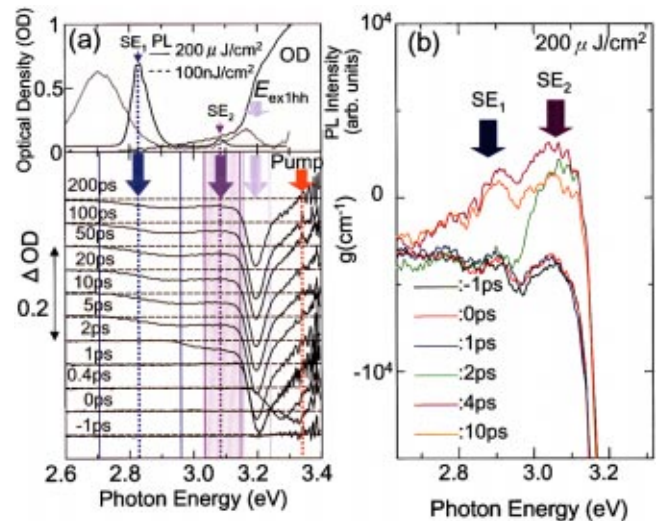


FIG. 5. (Color) (a) Differential optical density spectra as a function of time delay under $I_{ex}=200 \mu\text{J}/\text{cm}^2$ taken at sample (b) (blue LD). OD spectrum, SPE spectrum under $I_{ex}=100 \text{ nJ}/\text{cm}^2$, and SE spectrum under $I_{ex}=200 \mu\text{J}/\text{cm}^2$ are depicted in the figure. Two SE bands designated as SE_1 and SE_2 are also observed for the detection from the surface. (b) Dynamics of optical gain evaluated by the data in (a).

ated carriers rapidly (less than 1 ps) transferred to the LQL, and then relaxed to the localized tail within the time scale of several ps, giving rise to the optical gain.

The authors are grateful for the financial support of the Grant-in-Aid for Scientific Research from the Ministry of Education, Science, Sports and Culture. A part of this work was performed using the facility at the Venture Business Laboratory in Kyoto University (KU-VBL).

- ¹S. Nakamura, M. Senoh, S. Nagahama, N. Iwasa, T. Yamada, T. Matsushita, H. Kiyoku, and Y. Sugimoto, *Jpn. J. Appl. Phys., Part 2* **35**, L74 (1996).
- ²S. Nakamura, M. Senoh, S. Nagahama, T. Matsushita, H. Kiyoku, Y. Sugimoto, T. Kozaki, H. Umemoto, M. Sano, and T. Mukai, *Jpn. J. Appl. Phys., Part 2* **38**, L226 (1999).
- ³I. Akasaki, H. Amano, S. Sota, H. Sakai, T. Tanaka, and M. Koike, *Electron. Lett.* **32**, 1105 (1996).
- ⁴S. Nakamura, M. Senoh, S. Nagahama, N. Iwasa, T. Matsushita, and T. Mukai, *Appl. Phys. Lett.* **76**, 22 (2000).
- ⁵Y. Narukawa, Y. Kawakami, M. Funato, Sz. Fujita, Sg. Fujita, and S. Nakamura, *Appl. Phys. Lett.* **70**, 868 (1997).
- ⁶Y. Narukawa, Y. Kawakami, Sg. Fujita, and S. Nakamura, *Phys. Status Solidi A* **176**, 39 (1999).
- ⁷T. Deguchi, T. Azuhata, T. Sota, S. Chichibu, and S. Nakamura, *Mater. Sci. Eng., B* **50**, 251 (1997).
- ⁸G. Mohs, T. Aoki, M. Nagai, R. Shimano, M. Kuwata-Gonokami, and S. Nakamura, *Solid State Commun.* **104**, 643 (1997).
- ⁹A. Satake, Y. Masumoto, T. Miyajima, T. Asatsuma, and M. Ikeda, *Phys. Rev. B* **60**, 16660 (1999).
- ¹⁰Y. H. Cho, T. J. Schmidt, S. Bidnyk, G. H. Gainer, J. J. Song, S. Keller, U. K. Mishra, and S. P. DenBaars, *Phys. Rev. B* **61**, 7571 (2000).
- ¹¹Y. Narukawa, Y. Kawakami, Sz. Fujita, Sg. Fujita, and S. Nakamura, *Phys. Rev. B* **55**, R1938 (1997).
- ¹²Y. Narukawa, Y. Kawakami, Sg. Fujita, and S. Nakamura, *Phys. Rev. B* **59**, 10283 (1999).
- ¹³Y. Kawakami, Y. Narukawa, K. Omae, Sg. Fujita, and S. Nakamura, *Phys. Status Solidi A* **178**, 331 (2000).
- ¹⁴S. Nakamura, *Jpn. J. Appl. Phys., Part 2* **30**, L1705 (1991).
- ¹⁵Y. Narukawa, Ph.D. thesis, Kyoto University (2000).
- ¹⁶T. Takeuchi, S. Sota, M. Katsuragawa, M. Komori, H. Takeuchi, H. Amano, and I. Akasaki, *Jpn. J. Appl. Phys., Part 2* **36**, L382 (1997).